L06

Proceedings of the 5th International Conference on Inverse Problems in Engineering : Theory and Practice, Cambridge, UK, 11-15th July 2005

SOLUTION OF 3-DIMENSIONAL NONLINEAR INVERSE HEAT CONDUCTION BY USING A REDUCED NUMBER OF SENSORS

T. LOULOU[1] and E. ARTIOUKHINE[2]
[1]*Université de Bretagne Sud, Centre de Recherche LET2E, F-56321, Lorient, France*
e-mail: tahar.loulou@univ-ubs.fr
[2]*Institut FEMTO-ST, Departement CREST, 2 Avenue Jean Moulin, F-90000, Belfort, France*
e-mail: eugene.artioukhine@univ-fcomte.fr

Abstract - The goal of this work is to develop a numerical method and computational tools for solving a three-dimensional unsteady nonlinear inverse heat conduction problem of estimating the boundary condition at the heated surface of a cylindrically shaped solid. As additional information needed to solve the above inverse problem we use both temperature measurements collected on the opposite side given first by an infrared camera and second by a reduced number of sensors. The above inverse heat conduction problem is ill-posed which leads to a large sensitivity of the obtained numerical solution to measurement errors. In such a case a regularization has to be used to stabilize the solution. We use the iterative regularization method to build the numerical algorithm. According to the most effective version of the method applied to the inverse problem under analysis, the residual functional is minimized by means of the unconstrained conjugate gradient method. The unknown function of three variables is sought as a grid function which is considered as an element of L_2 space. To compute the residual functional gradient, the adjoint problem is solved. The linear approximation of the descent parameter is used in the algorithm which is computed with the use the direct problem in variations. The regularizing residual (discrepancy) criterion is utilized to stop the iterative process. The performance and the solution exactness of the inverse heat conduction problem under consideration obtained by the proposed algorithm are analyzed by analyzing different heat flux test cases with different shapes in time and space. Then an inspection of the reduction of temperature measurement points is analyzed. Indeed, instead of using surface measurement (measurement points equal computation grids which corresponds to an infrared camera) the measurement points are reduced progressively. The results of the analyzed test cases show a good accuracy and robustness of obtained solutions when a reduced number of temperature sensors is used.

1. INTRODUCTION

Linear and nonlinear inverse heat conduction problems have been analyzed very intensively during the last thirty five years. There are excellent books on this subject [2, 6, 10, 15, 21]. For two-dimensional linear and nonlinear inverse problems, much progress have been achieved in the last decade [1, 3, 9, 13, 17–19]. It should noted that two-dimensional heat conduction problems have been much more extensively investigated than three-dimensional inverse problems. Indeed, the solution of three-dimensional nonlinear inverse problems is very time consuming and requires a large random access memory. This is one of the main reasons why, to date, just a few works are published in this promising direction of inverse problems. The last developed studies were performed in [4,9,11,12,16,25,26].

The main goal of this work is to develop a numerical method and computational tools for solving the three-dimensional unsteady nonlinear inverse heat conduction problem of estimating the boundary conditions at the heated surface of a hollow half-cylinder. As inverse heat conduction problems are ill-posed this leads to a large sensitivity in the obtained numerical solution to the measurement errors. That is why a regularization is needed to stabilize numerical solutions. The inverse problem is to estimate a heat flux density evolution at the external surface. Measurements are simulated numerically at the internal surface of the half-cylinder. The performance and the error analysis of the inverse heat conduction problem solutions obtained by the proposed algorithm are analyzed by considering two heat flux test cases in function of space and time. Indeed, a nonlinear three-dimensional analysis was conducted to analyze the performance of the iterative regularization method and its capability for experimental data processing.

2. INVERSE PROBLEM

The geometry of the solid considered in this paper consists of a finite, hollow, half-cylinder with inside radius r_0, outside radius r_1, and length z_1. The lateral surface of the half-cylinder is submitted to an unknown heat flux while all others boundaries are kept insulated. The nonlinear heat conduction process in the cylindrical coordinate

system, i.e. $T(r, \phi, z, t)$, is described by the following set of equations:

$$c\frac{\partial T}{\partial t} = \frac{1}{r}\frac{\partial}{\partial r}\left(r\,k\frac{\partial T}{\partial r}\right) + \frac{1}{r^2}\frac{\partial}{\partial \phi}\left(k\frac{\partial T}{\partial \phi}\right) + \frac{\partial}{\partial z}\left(k\frac{\partial T}{\partial z}\right) \tag{1}$$

$$r_0 < r < r_1 \quad 0 < \phi < \pi \quad 0 < z < z_1 \quad t_0 < t \leq t_f$$

$$\frac{\partial T(r_0, \phi, z, t)}{\partial r} = 0 \qquad 0 \leq \phi \leq \pi \qquad 0 \leq z \leq z_1 \qquad t_0 < t \leq t_f \tag{2}$$

$$k\frac{\partial T(r_1, \phi, z, t)}{\partial r} = q(\phi, z, t) \qquad 0 \leq \phi \leq \pi \qquad 0 \leq z \leq z_1 \qquad t_0 < t \leq t_f \tag{3}$$

$$\frac{\partial T(r, \phi, 0, t)}{\partial z} = 0 \qquad r_0 \leq r \leq r_1 \qquad 0 \leq \phi \leq \pi \qquad t_0 < t \leq t_f \tag{4}$$

$$\frac{\partial T(r, \phi, z_1, t)}{\partial z} = 0 \qquad r_0 \leq r \leq r_1 \qquad 0 \leq \phi \leq \pi \qquad t_0 < t \leq t_f \tag{5}$$

$$T(r, \phi, z, 0) = T_i \qquad r_0 \leq r \leq r_1 \qquad 0 \leq \phi \leq \pi \qquad 0 \leq z \leq z_1 \tag{6}$$

When the applied heat flux density $q(\phi, z, t)$ is known, the presented model (direct problem) is used to predict the temperature field. When the applied heat flux density $q(\phi, z, t)$ is unknown, but additional information in the form of temperature measurements is available, the previous problem can be solved to estimate both the temperature distribution and the applied heat flux density by solving the inverse heat conduction problem.

In this work, we suppose that temperature measurements are carried out at the internal cylindrical surface, i.e. at radius r_0, which could represent a difficult inverse problem if the thickness $r_1 - r_0$ is important. In this case, the measurement results can be presented as follows :

$$T_m(r_0, \phi, z, t) = Y(\phi, z, t) \tag{7}$$

In addition, the number of discrete measurement points at the measurement surface is large enough so that the function $f(\phi, z, t)$ can be presented as a piece-wise linear continuous function. The inverse problem under analysis is to estimate the heat flux density $q(\phi, z, t)$ by using the the direct problem (1) to (6) and the temperature measurements (7).

3. ALGORITHM

The iterative regularization method is used to build a numerical algorithm of the above inverse problem. The method is based on a variational formulation of an inverse problem. First, this leads to the introduction of the residual functional which determines the "distance" between the response of the system computed by solving the direct problem according to the measurement scheme and the measured response. In the majority of practical applications, the residual functional (the distance between the two responses) is defined in the Hilbert space L_2 of functions squared integrable. For the inverse problem analyzed in this paper we use the continues form of the residual functional and is defined as

$$J(q) = \int_0^{t_f}\int_0^{\pi}\int_{z_o}^{z_1} \left[\Delta(\phi, z, t)\right]^2 dz\, d\phi\, dt \tag{8}$$

where $\Delta(\phi, z, t)$ represents the distance $T(d, \phi, z, t; q) - Y(\phi, z, t)$, $T(d, \phi, z, t)$ designates the temperature evolution computed at the measurement surface $S(r_0, \phi, z)$ and $Y(\phi, z, t)$ represents the measured temperature evolution at the same surface, respectively. Second, it is necessary to define what kind of function is being sought, i.e. the space to which the unknown function belongs should be specified. In our inverse problem the desired function sought is a grid function and is considered as an element of the Hilbert space L_2. Third, it has been shown for linear general inverse problems (in operator form) [2,5] that one very effective approach to obtain a stable solution of inverse problems is to use unconstrained, on the desired function, gradient-type numerical methods of the first kind for the problem of the residual functional minimization given by

$$J(q) = \left\| T(d, \phi, z, t; q) - f(\phi, z, t) \right\|^2 \rightarrow \min_{q \in L_2} \tag{9}$$

under constraints on the temperature given by all equations of the direct problem (1) to (6), because the temperature in the specimen can not be fixed arbitrarily. It is computed from the direct problem.

The most efficient gradient-type numerical method is the conjugate gradient method [23]. The successive improvements of the desired function are built as follows :

$$q^{s+1}(\phi, z, t) \;=\; q^{s}\,(\phi, z, t) \;+\; \gamma^{s}\, D^{s}(\phi, z, t) \tag{10}$$

where s is the iteration number ($s = 0$ is the initial guess), γ^s is the descent parameter, and $D^s(\phi, z, t)$ is the descent direction, and $q^0(\phi, z, t)$ is initial approximation of the unknown function given a priori. The descent direction is given by:

$$D^{s}(\phi, z, t) \;=\; -\,J'^{s}(\phi, z, t) \;+\; \beta^{s}\, D^{s-1}(\phi, z, t) \tag{11}$$

where the parameter β^s is given by formula (12) when using the Polak-Ribière version, i.e.

$$\beta^{s} \;=\; \frac{\displaystyle\int_0^{t_f}\int_0^{\pi}\int_{z_o}^{z_1} X(\phi, z, t)\, J'^{s}(\phi, z, t)\, dz\, d\phi\, dt}{\displaystyle\int_0^{t_f}\int_0^{\pi}\int_{z_o}^{z_1} \left[J'^{s-1}(\phi, z, t)\right]^2 dz\, d\phi\, dt} \tag{12}$$

where $X(\phi, z, t) = J'^{s}(\phi, z, t) - J'^{s-1}(\phi, z, t)$, or expression (13) when using the Fletcher-Reeves version of the conjugate gradient method [23] :

$$\beta^{s} \;=\; \frac{\displaystyle\int_0^{t_f}\int_0^{\pi}\int_{z_o}^{z_1} \left[J'^{s}(\phi, z, t)\right]^2 dz\, d\phi\, dt}{\displaystyle\int_0^{t_f}\int_0^{\pi}\int_{z_o}^{z_1} \left[J'^{s-1}(\phi, z, t)\right]^2 dz\, d\phi\, dt} \tag{13}$$

In the absence of measurement noise (this is a typical case for optimal control problems), numerical experiments show that the above iterative process can be repeated until the function $q(\phi, z, t)$ satisfies the following stopping criterion:

$$\left|\frac{q^{s+1}(\phi, z, t) \;-\; q^{s}(\phi, z, t)}{q^{s+1}(\phi, z, t)}\right| \;\leq\; \varepsilon, \tag{14}$$

where ε is a small number ($10^{-4} \sim 10^{-5}$). This property of the conjugate method is very useful. It is widely used to verify numerical algorithms and programs for solving test inverse problems without noise.

As it is well known, inverse problems of experimental data processing cannot be solved as easily as direct problems because of their inherent ill-posed character. Indeed, their solutions don't depend continuously on the data . Small changes in the input data can produce large deviations in the solution [2, 6, 24]. The iterative regularization method [2, 4] is used to stabilize the solution of the studied inverse problem. The idea of the method is based on the use the discrepancy principal as a stopping criterion for the iterative process:

$$J(q) \approx \delta^2 \tag{15}$$

where δ^2 is the generalized measurement error computed in the same space as the residual functional.

$$\delta^2 \;=\; \int_0^{t_f}\int_0^{\pi}\int_{z_o}^{z_1} \sigma^2(\phi, z, t)\, dz\, d\phi\, dt \tag{16}$$

and $\sigma^2(\phi, z, t)$ is the standard deviation of measured temperatures obtained using smoothing techniques for example. In other words, this approach is part of the regularization method and gives regularizing algorithms.

The minimization of the residual functional (8) by the conjugate gradient method requires the computation of its gradient with respect to the desired function $q(\phi, z, t)$ in the space L_2. There are several ways to derive the gradient of $J(q)$. One way is to use the calculus of variations and Lagrange multipliers method [5]. A similar approach have been used in [1]. Finally, all methods lead to the adjoint problem which is used to compute the residual functional gradient. The same approach is applied in this paper. It can be shown that the residual functional gradient in the space L_2 is given by:

$$J'(\phi, z, t) \;=\; \psi(r_1, \phi, z, t) \tag{17}$$

where $\psi(r_1, \phi, z, t)$ is solution of the "adjoint problem" given by the following set of equations:

$$-\,c\,\frac{\partial \psi}{\partial t} \;=\; k\,\frac{\partial^2 \psi}{\partial r^2} \;+\; \frac{k}{r}\,\frac{\partial \psi}{\partial r} \;+\; \frac{k}{r^2}\,\frac{\partial^2 \psi}{\partial \phi^2} \;+\; k\,\frac{\partial^2 \psi}{\partial z^2} \;+\; \frac{k}{r^2}\psi \;+\; S(r, \phi, z, t) \tag{18}$$

$$r_0 < r < r_1 \quad 0 < \phi < \pi \quad 0 < z < z_1 \quad t_0 \leq t < t_f \tag{19}$$

$$\frac{\partial \psi(r_0, \phi, z, t)}{\partial r} = 0 \qquad 0 \leq \phi \leq \pi \qquad 0 \leq z \leq z_1 \qquad t_0 < t \leq t_f \tag{20}$$

$$\frac{\partial \psi(r_1, \phi, z, t)}{\partial r} = 0 \qquad 0 \leq \phi \leq \pi \qquad 0 \leq z \leq z_1 \qquad t_0 < t \leq t_f \tag{21}$$

$$\frac{\partial \psi(r, \phi, 0, t)}{\partial z} = 0 \qquad r_0 \leq r \leq r_1 \qquad 0 \leq \phi \leq \pi \qquad t_0 < t \leq t_f \tag{22}$$

$$\frac{\partial \psi(r, \phi, z_1, t)}{\partial z} = 0 \qquad r_0 \leq r \leq r_1 \qquad 0 \leq \phi \leq \pi \qquad t_0 < t \leq t_f \tag{23}$$

$$k \frac{\partial \psi(d, \phi, z_1, t)}{\partial z} = \qquad r_0 \leq r \leq r_1 \qquad 0 \leq \phi \leq \pi \qquad t_0 < t \leq t_f \tag{24}$$

$$\psi(r, \phi, z, t_f) = 0 \qquad r_0 \leq r \leq r_1 \qquad 0 \leq \phi \leq \pi \qquad 0 \leq z \leq z_1 \tag{25}$$

where the source term $S(r, \phi, z, t)$ is equal to $\Delta(\phi, z, t) \times \delta(\phi - \phi_i) \times \delta(z - z_i)$ and where $\delta(.)$ is the Dirac delta function. The descent parameter γ^s, which characterizes the step size in going from q^s to q^{s+1}, is obtained at each iteration by minimizing $J(q^{s+1})$ given by eqn. (8), with respect to γ^s. For our inverse problem the following result is obtained:

$$\gamma^s = - \frac{\int_0^{t_f} \int_0^{\pi} \int_{z_o}^{z_1} \Delta(\phi, z, t)\, \upsilon(d, \phi, z, t)\, dz\, d\phi\, dt}{\int_0^{t_f} \int_0^{\pi} \int_{z_o}^{z_1} [\upsilon(d, \phi, z, t)]^2\, dz\, d\phi\, dt} \tag{26}$$

In the above formula, $\upsilon(r, \phi, z, t)$ is the solution of the "variation problem" defined by the following system of equations :

$$\frac{\partial (c\upsilon)}{\partial t} = \frac{1}{r} \frac{\partial}{\partial r} \left[r \frac{\partial (k\upsilon)}{\partial r} \right] + \frac{1}{r^2} \frac{\partial}{\partial \phi} \left[\frac{\partial (k\upsilon)}{\partial \phi} \right] + \frac{\partial}{\partial z} \left[\frac{\partial (k\upsilon)}{\partial z} \right] \tag{27}$$

$$r_0 < r < r_1 \quad 0 < \phi < \pi \quad 0 < z < z_1 \quad t_0 < t \leq t_f \tag{28}$$

$$- \frac{\partial (k\upsilon)}{\partial r}(r_0, \phi, z, t) = 0 \qquad 0 \leq \phi \leq \pi \qquad 0 \leq z \leq z_1 \qquad t_0 < t \leq t_f \tag{29}$$

$$- \frac{\partial (k\upsilon)}{\partial r}(r_1, \phi, z, t) = \Delta q(\phi, z, t) \qquad 0 \leq \phi \leq \pi \qquad 0 \leq z \leq z_1 \qquad t_0 < t \leq t_f \tag{30}$$

$$- \frac{\partial (k\upsilon)}{\partial z}(r, \phi, 0, t) = 0 \qquad r_0 \leq r \leq r_1 \qquad 0 \leq \phi \leq \pi \qquad t_0 < t \leq t_f \tag{31}$$

$$- \frac{\partial (k\upsilon)}{\partial z}(r, \phi, z_1, t) = 0 \qquad r_0 \leq r \leq r_1 \qquad 0 \leq \phi \leq \pi \qquad t_0 < t \leq t_f \tag{32}$$

$$\upsilon(r, \phi, z, 0) = 0 \qquad r_0 \leq r \leq r_1 0 \leq \phi \leq \pi \qquad 0 \leq z \leq z_1 \tag{33}$$

where $T(r, \phi, z, t)$ is the solution of the "direct problem" given in eqns (1)-(4), and $f(\phi, z, t)$ is the measured temperatures at the surface defined by $r = d$, $0 \leq \phi \leq \pi$, and $0 \leq z \leq z_1$. In the variation problem, the term $\Delta q(\phi, z, t)$ is defined by $\Delta q(\phi, z, t) = D^s(\phi, z, t)$, the descent direction.

Minimization procedure : The minimization procedure can be implemented following the traditional scheme [2, 14]. At each iteration, we must solve three problems, the "*direct*", the "*adjoint*" and the "*variation*" problems. As these problems are similar, we can use the same algorithm to solve them numerically. These problems are solved numerically using the control volume method [22] and the implicit fractional-step time scheme proposed by Brian [7]. This scheme is given by :

$$\begin{aligned} \frac{T^* - T^n}{\Delta t/2} &= \Delta_r^2 T^* + \Delta_\phi^2 T^n + \Delta_z^2 T^n \\ \frac{T^{**} - T^n}{\Delta t/2} &= \Delta_r^2 T^* + \Delta_\phi^2 T^{**} + \Delta_z^2 T^n \\ \frac{T^{n+1} - T^{**}}{\Delta t/2} &= \Delta_r^2 T^* + \Delta_\phi^2 T^{**} + \Delta_z^2 T^{n+1} \end{aligned} \tag{34}$$

where Δ_r^2, Δ_ϕ^2, and Δ_z^2 are the second finite difference operators in r, ϕ, and z directions. By using this scheme only, a three-diagonal matrix inversion is carried out with the Thomas algorithm at each time step [8].

4. RESULTS

Before presenting the analysis of the inverse problem under hand, the numerical tool developed to solve the direct, variation and adjoint problems is investigated. To check the solution accuracy of the direct problem by the fractional scheme time, eqns (34), numerical results are compared with those obtained analytically. Indeed by prescribing a constant heat flux over ϕ, z, and t, i.e. $q(\phi, z, t) = q_c = 1$, and taking constant thermophysical properties $c = k = 1$, an analytical solution for this three dimensional linear problem can be derived [20]. Numerical simulations have shown that an excellent agreement between analytical and numerical solutions is obtained when the Fourier number defined as

$$Fo = \frac{\alpha \Delta t}{(\Delta r)^2} + \frac{\alpha \Delta t}{(\Delta \phi)^2} + \frac{\alpha \Delta t}{(\Delta z)^2} \tag{35}$$

is taken to be less than or equal to 1. The quantities Δr, $\Delta \phi$, Δz, and Δt are, respectively, the radius, angular, longitudinal, and time steps, and α represents the thermal diffusivity. The comparison tests were conducted with the following thermal and geometric characteristics

$$\begin{array}{ccccccccc} & & k(T) = 1.0 & & c(T) = 1.0 & & T_i = 1.0 & & \\ r_o = 0.5 & r_1 = 1.0 & & \phi_o = 0 & & \phi_1 = \pi & & z_o = 0 & z_1 = 1.0 \quad t_f = 1.0 \end{array} \tag{36}$$

By taking the spatial and temporal resolution as : $n_r \times n_\phi \times n_z \times n_t = 11 \times 11 \times 11 \times 401$, the value of the resulting Fourier number is 1.275 and the maximum relative error between analytical and numerical solution is about 0.4 %. If we keep the above same temporal resolution, but double the space grid ($n_r \times n_\phi \times n_z \times n_t = 21 \times 21 \times 21 \times 401$), the Fourier number becomes 5.10 and the relative error increases to 1 %. A more fine spatial resolutions have been tested and give relatively bad results. The smaller space the resolution the bigger the estimation error. In the remaining parts of this paper the first spatial and time resolution are used in solving the inverse problem under consideration. The choice of this resolution is motivated by a compromise between the accuracy of calculations and the reduction of the computing time.

To illustrate the application of the iterative regularization method for the three-dimensional transient nonlinear inverse problem, we consider two examples of estimating numerically the time and space-wise variation of an applied heat flux. The two cases use temperature fields measured on the back side of the half cylinder, i.e. over the internal surface $S(r_0, \phi, z)$. The analytical expression of test case 1 is given by :

$$q(\phi, z, t) = \frac{1 - \sin\left[\sqrt{\phi^2 + t^2}\right] \sin\left[\sqrt{\phi^2 + t^2}\right]}{\left[1 + 10(t^2 + \phi^2)\right]\left[1 + 10(t^2 + \phi^2)\right]} \tag{37}$$

The second test case is expressed by :

$$q(\phi, z, t) = \frac{t \exp(-t^2 - \phi^2)}{q_{max}} \tag{38}$$

where q_{max} is 0.43. The presentation of the results in three dimensions (ϕ, z, t), could be confusing and difficult to understand. This is the reason why in this study we will present our numerical simulations in only two dimensions (ϕ, t) or (z, t). To do that we can consider that the heat flux presents the same variation following the length z or the angle ϕ as shown by expressions (37) and (38). The first test is more difficult than the second one because it presents a sharp Gaussian variation which can be compared to step variation in one dimensional problems. The second case simulates a combined heating and cooling phenomenon occurring over the external surface during the time interval [0, t_f].

A delta Fourier number (dimensionless time step) based on the sensor depth to the active surface, the thermal diffusivity α, and the time step Δt is introduced to characterize the degree of difficulty of the analyzed inverse heat conduction problem. It is defined as follows :

$$\Delta Fo = \frac{\alpha \, \Delta t}{[r_1 - r_0]^2} \tag{39}$$

The ΔFo of the presented test cases was taken as 0.01, which is of the same order of magnitude or less as those presented in the literature [2, 6]. The thermophysical properties of the nonlinear model are given by :

$$k(T) = 1.0 + 4.0T^2 \qquad c(T) = 1/[1 + 2T] \tag{40}$$

The quality of the estimation of the desired function $q(\phi, z, t)$ is quantified through the computed error according to the formula :

$$\epsilon = \frac{\int_0^{t_f} \int_0^{z_1} \int_0^{\pi} \left[\hat{q}(\phi, z, t) - q(\phi, z, t)\right]^2 d\phi \, dz dt}{\int_0^{t_f} \int_0^{z_1} \int_0^{\pi} \left[\hat{q}(\phi, z, t)\right]^2 d\phi \, dz dt} \tag{41}$$

and the root mean square error (*rms*) given by :

$$\varrho = \sqrt{\frac{1}{n_\phi n_z n_t} \sum_{i=1}^{n_\phi} \sum_{j=1}^{n_z} \sum_{k=1}^{n_t} \left[\hat{q}_{ijk} - q_{ijk}\right]^2} \tag{42}$$

where $\hat{q}(\phi, z, t)$ and $q(\phi, z, t)$ are respectively the exact and recovered functions ($q_{ijk} = q(\phi_i, z_j, t_k)$).

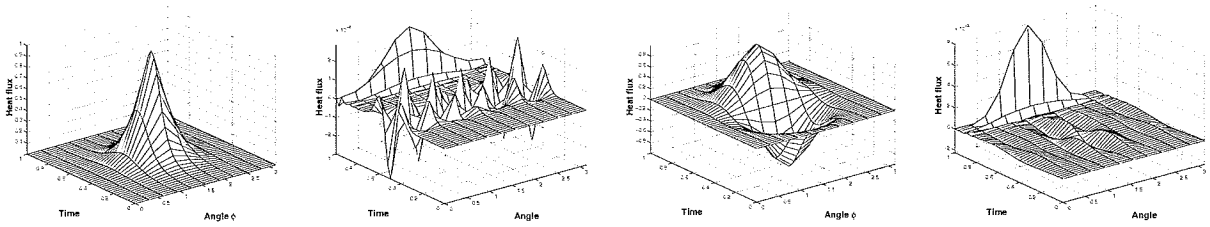

(a) Recovered test case 1. (b) Exact - recovered : 1. (c) Recovered test case 2. (d) Exact - recovered : 2.

Figure 1. Shapes of recovered heat flux obtained with errorless data for two different test cases where $\Delta Fo = 0.01$.

Errorless data : All of the presented test cases were first performed with exact (errorless) and secondly with noised data starting in both cases with a null initial guess, that is $q^0(\phi, z, t) = 0$. The computation results with errorless data and the difference between recovered and prescribed heat flux shapes are depicted in Figure 1. For both cases the recovered results reveal almost no difference from the original (exact profile) applied heat flux density. However to obtain these results the optimization method needs an important number of iterations which results in a considerable computing time. Results of test case 1 were obtained after 2368 iterations which corresponds approximately to 56 min CPU time. As we are dealing with exact measurements, the eqn. (14) is used as a stopping criterion and the prescribed value of ε was taken as 10^{-5} for both cases. The obtained *rms* error is equal to 1.97×10^{-4} and the resulting estimation error ϵ is about $0.1\,\%$ for the test case 1. Figures 1-a and 1-b summarize the estimations results. The recovered heat flux, for test case 2, shown in Figure 1-c is obtained within 511 iterations and 12 min CPU time. The corresponding obtained *rms* error is equal to 9.96×10^{-4} and the relative estimation error is about $0.001\,\%$. This small error is better viewed through Figure 1-d which displays the difference between the exact and recovered heat flux shape. In Figure 1-d the sharp variation near the final time t_f is due to the inherent null condition of the adjoint problem stated by eqn. (25). The variation of residual functional and relative estimation error as a function of iteration number are displayed in Figure 2 for both cases. We observe that the convergence is fast in the first steps and then slows down as the result approaches the exact solution. The reduction of the estimation error shows also the same behavior and decreases below $0.01\,\%$ in the first hundred iterations for the second test.

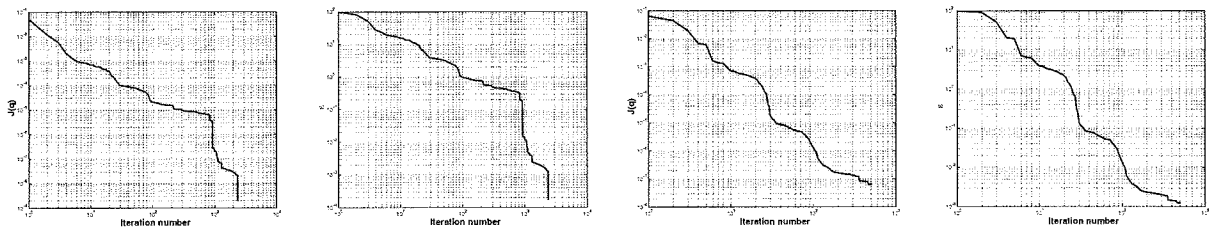

(a) Residual functional : 1. (b) Estimation error : 1. (c) Residual functional : 2. (d) Estimation error : 2.

Figure 2. Evolution of the residual functional $J(q)$ and the relative estimation error ϵ as a function of iteration number for both cases : 1 and 2 with errorless data.

Data with noise : The measured temperatures are simulated by the following expression

$$Y(\phi, z, t) = T_x(r_0, \phi, z, t) + \omega\, T_{max}\, \Delta_{max} \tag{43}$$

where $T_x(r_0, \phi, z, t)$ is the exact temperature. In fact to the theoretical temperature profile $T_x(r_0, \phi, z, t)$ we add white and normal noise. The perturbation is defined as $\omega\, T_{max}\, \Delta_{max}$, where ω is a random number generator $[-1, +1]$, T_{max} is the maximum temperature value over the heated surface, and Δ_{max} is the magnitude of the perturbation (in %). Numerical test cases presented in this paper were analyzed by taking the parameter Δ_{max} equal to 1% and 4%. The stopping criteria in this case is based on the iterative regularization method, eqn. (15). The iterative process (eqn.(10)) is stopped when the value of the functional residual reaches approximately the δ^2

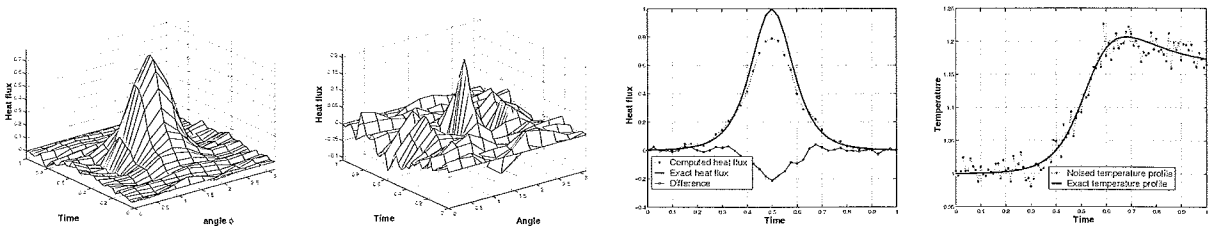

(a) Recovered heat flux. (b) Exact - recovered. (c) Heat flux at point : p. (d) Temperature at point : p.

Figure 3. Results for test case 1. Results obtained with noised data. Measurements performed over the internal surface at $r = r_o$. Noise level taken as 1% of T_{max} and $\Delta Fo = 0.01$.

value, see eqn.(15). As the residual functional value $J(q)$ can never be precisely equal to the value of the integrated error δ^2, the iterative process can be stopped just before or just after reaching this value.

Test case 1 : We have chosen a Gaussian variation over time for the heat flux in the first example. The final time is taken as $t_f = 1.$ and the initial temperature as $T_i = 0$. The heat flux is supposed to be constant over z (no variation following z). As the temperature measurements are collected over the internal surface of the half cylinder, i.e $S(r_0, \phi, z)$ gives a delta Fourier number 0.01. With regard to the literature [2,5,6], this case represents a difficult example due to the error amplification character of ill-posed problems. The maximum value of heat flux density in this case is about 1 during a short time period. In Figure 3 we present the different results obtained with a noise level $\Delta_{max} = 1\,\%$. The shown results underline the difficulties of the algorithm to overcome the instabilities due to the noisy data and especially at the peak value of the heat flux, see Figure 3-b. As presented in Figure 3-c, the largest difference between exact and computed values of the heat flux density is located at the point **p** located over the heated surface at ($r = r_1$, $\phi = \pi/2$, $z = z_1/2$). The order of this difference is around 20 % of the maximum value of the heat flux. Except for the summit of the Gaussian, the results around it are in good agreement with the exact values. The exact and simulated noised temperatures at the point **p** are depicted in Figure 3-d. Inspecting Figures 3-d and 3-b we observe that the estimation error of the unknown heat flux is still small in comparison with the level of added noise.

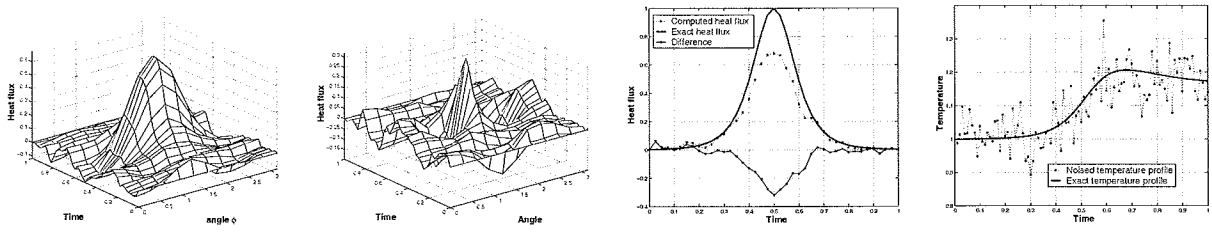

(a) Recovered heat flux. (b) Exact - recovered. (c) Heat flux at point : p. (d) Temperature at point : p.

Figure 4. Results for test case 1. Results obtained with noised data. Measurements performed over the internal surface at $r = r_o$. Noise level taken as 4% of T_{max} and $\Delta Fo = 0.01$.

The same test case was solved for $\Delta_{max} = 2\%$ and $\Delta_{max} = 4\%$ which means a higher noise level. Figure 4-d gives an idea of the nature of the used simulated temperatures for the highest noise level. The recovered results are still in good enough agreement with the exact ones except around the peak of the considered Gaussian. At point **p** the difference between exact and reconstructed heat flux is more pronounced (about 25 %) than the above example (noise level = 1 %) but not multiplied by 4 as done with the noise level. This observation confirms that this example is difficult in itself besides the error introduced by the measurement errors. From the presented case, we conclude that reliable inverse results can still be obtained when measurements errors are considered with a relatively high noise level. The *rms* error, computing time, estimation error, and iteration number required to solve the inverse problem are reported in Table 1 for errorless data and noised data with different noise level.

Test case 2 : The developed algorithm was tested with second example. As in the above case the measurements are supposed to be taken over the internal surface. The delta Fourier remains unchanged at 0.01. In this case the maximum heat flux is chosen as $q_{max} = 1$. The second example supposes that there is negative variation following t for the heat flux (cooling phenomenon). Figure 5 summarizes the recovered results when we use noisy data with a maximum amplitude of 1 %. The shown results were obtained in 38 iterations with a CPU time of 54 s. The estimated heat flux density, Figure 5-a, presents a small roughness at its basis but is still stable with respect to the input data. The obtained results confirm the efficiency of the developed algorithm. The difference between the exact and recovered heat flux density values for this case is presented in Figure 5-b. The residuals are of the same order of magnitude as those observed in the first example. The estimation error is around 0.66 % according to

Table 1. Summary of results for test 1 and 2 where τ_c designates the computing time and $It.\ N.$ represents the iteration number.

$\Delta_{max}(\%)$	Parameter	Unit	Test 1	Test 2
1.0	ϱ		0.0382	0.0249
	ϵ	%	6.061	0.660
	τ_c	s	47	53
	$It.\ N.$		34	38
2.0	ϱ		0.0518	0.0430
	ϵ	%	10.680	1.740
	τ_c	s	41	43
	$It.\ N.$		30	31
4.0	ϱ		0.0614	0.0585
	ϵ	%	15.528	3.428
	τ_c	s	29	33
	$It.\ N.$		21	24

expression (41) which is a little high due to the weak space modeling ($n_r \times n_\phi \times n_z$) of the heat flux density. In fact, a greater space resolution would be better to represent correctly the space variation for both test cases without missing the constraint established in the beginning of the results section about the Fourier number ($Fo \approx 1$). For example if we double the number of grid spaces and keep the same order of Fourier number, the time step should be chosen as small as 0.00049 which results in 2041 time steps. This new space and time grid resolution requires a considerable computer memory.

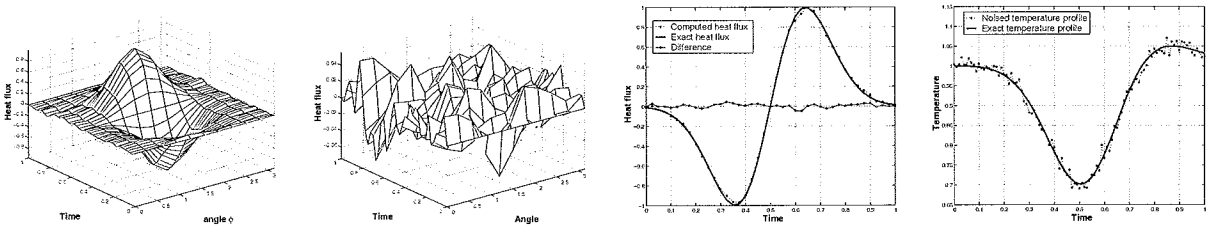

(a) Recovered heat flux. (b) Exact - recovered. (c) Heat flux at point : p. (d) Temperature at point : p.

Figure 5. Results for test case 2. Results obtained with noised data. Measurements performed over the internal surface at $r = r_o$. Noise level taken as 1% of T_{max} and $\Delta Fo = 0.01$.

The time variation of the heat flux at the point **p**, located at ($r = r_1$, $\phi = \pi/2$, $z = z_1/2$), is plotted in Figure 5-c. The comparison between the exact and recovered heat flux profiles shows an acceptable agreement and the estimated heat flux becomes closer to the exact one. The estimated results show less roughness in comparison with those presented in the first test case. This "weak" roughness is probably due to the relatively smooth variation of the heat flux. The same Figure 5-c presents also the difference between theoretical and estimated heat flux density profile, at the point **p**, for the second case when using noisy data. Regarding the displayed residuals, Figure 5-c, the recovered results are more accurate than those observed in the first case which is consistent with the physics of the problem. The nature of "measured" temperatures used in solving this inverse problem is shown in Figure 5-d. It represents the exact and simulated measured temperature at the point **p**.

Figure 6 summarizes graphically the obtained results in the second test case where the simulated data are perturbed with level noise of 4 %. Figure 6-d gives an idea on the temperature profiles used in this second simulation. The recovered heat flux at the point **p** located at ($r = r_1$, $\phi = \pi/2$, $z = z_1/2$) is presented in Figure 6-c. The computed surface heat flux fits the exact profile in a satisfactory way. The difference between them at the point

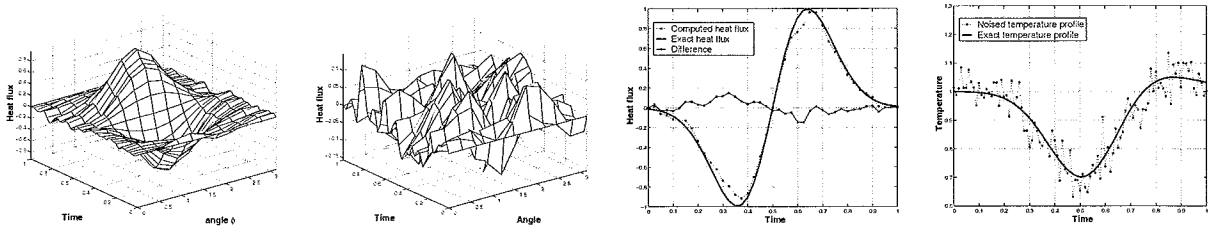

(a) Recovered heat flux. (b) Exact - recovered. (c) Heat flux at point : p. (d) Temperature at point : p.

Figure 6. Results for test case 2. Results obtained with noised data. Measurements performed over the internal surface at $r = r_o$. Noise level taken as 4% of T_{max} and $\Delta Fo = 0.01$.

p is shown in the same figure. Here again the estimated results are acceptable and underline the efficiency of the developed iterative method.

Table 1 gives a summary of the obtained results for both test cases. In all the presented numerical simulations, no *a priori* information on the unknown evolution to be recovered is used and the initial guess of the heat flux density was set always equal to zero.

5. CONCLUSIONS

The objective of the present work was to show the application of the conjugate gradient method, coupled to the iterative regularization method, for estimating three-dimensional heat flux by using a nonlinear heat conduction model. This study was accomplished through the use of the adjoint problem to compute the gradient combined with the conjugate gradient algorithm to minimize the residual functional. The algorithm was successfully implemented and relatively correct results were obtained with noisy measurements. It was shown that the obtained results are still in the range of the desired estimation error. Further numerical verification tests will be conducted to show the efficiency of this algorithm in the presence of high and low time and space frequencies in the heat flux density evolution.

REFERENCES

1. R. Abou Khachfe and Y. Jarny, Numerical solution of 2-d non-linear inverse heat conduction problems using finite element techniques. *Numer. Heat Transfer, Part B* (2000) **37**, 45-68.

2. O.M. Alifanov, *Inverse Heat Transfer Problems*, Springer-Verlag, Berlin, 1994.

3. O.M. Alifanov and Y.V. Egorov, Algorithms and results of solving the inverse heat conduction problem in a two-dimensional formulation. *J. Eng. Phys.* (1985) **48**(4), 489-496.

4. O.M. Alifanov and A.V. Nenarokomov, Three dimensional boundary inverse heat conduction problem for regular coordinates. *Inverse Problems Eng.* (1999) **7**, 335-362.

5. O.M. Alifanov, E.A. Artyukhin and S.V. Rumyantsev, *Extreme Methods of Solving Ill-Posed Problems and theirs Applications to Inverse Heat Transfer Problems*, Begell House, New York, 1995.

6. J.V. Beck, B. Blackwell and C.R. St. Clair, *Inverse Heat Conduction. Ill-Posed Problems*, Wiley Interscience, New York, 1985.

7. P.L.T. Brian, A finite-difference method of higher order accuracy for solution of three-dimensional transient heat conduction. *AIChE J.* (1961) **7**(3),367-370.

8. B. Carnahan, H.A. Luther and J.O. Wilkes, *Applied Numerical Methods*, Krieger, Florida, 1990.

9. K.J. Dowding and J.V. Beck, A sequential gradient method for the inverse heat conduction problem (ihcp). *ASME J. Heat Transfer* (1999) **121**, 300-306.

10. E. Hensel, *Inverse Theory and Applications for Engineers*, Prentice-Hall, New Jersey, 1991.

11. C.H. Huang and W.C. Chen, A three dimensional inverse forced convection problem in estimating surface heat flux by conjugate gradient method. *Int. J. Heat Mass Transfer* (2000) **43**(2), 3171-3181.

12. C.H. Huang and S.P. Wang, A three dimensional inverse heat conduction problem in estimating surface heat flux by conjugate gradient method. *Int. J. Heat Mass Transfer* (1999) **42**, 3387-3403.

13. S.K. Kim, J. Lee and W.I. Lee, A solution method for nonlinear three dimensional inverse heat conduction problem using the sequential gradient method combined with cubic-spline function specification. *Numer. Heat Transfer, Part B* (2003) **43**, 43-61.

14. T. Loulou and E.P. Scott, Estimation of 3-Dimensional heat flux from surface temperature measurements by using iterative regularization method. *Heat Mass Transfer* (2003) **39**, 435-443.

15. D.A. Murio, *The Mollification Method and the Numerical Solution of Ill-Posed Problems*, John Wiley, New York, 1993.

16. D. Nortershauser and P. Millan, Resolution of a three-dimensional unsteady inverse problem by sequential method using parameter reduction and infrared thermography measurements. *Numer. Heat Transfer, Part A* (2000) **37**, 587-611.

17. A.M. Osman and J.V. Beck, Nonlinear inverse problem for estimation of time and space dependent heat transfer coefficients. *AIAA J. Thermophys. Heat Transfer* (1989) **3**, 146-152.

18. A.M. Osman and J.V. Beck, Investigation of transient heat transfert coefficients in quenching experiments. *ASME J. Heat Transfer* (1990) **112**, 843-848.

19. A.M. Osman, K.J. Dowding and J.V. Beck, Numerical solution of the general two-dimensionnal inverse heat conduction problem (ihcp). *ASME J. Heat Transfer* (1997) **119**, 38-45.

20. M.N. Ozişik, *Heat Conduction*, John Wiley & Sons, New York, 1993.

21. M.N. Ozişik and H.R.B. Orlande, *Inverse Heat Transfer : Fundamentals and Applications*, Taylor and Francis, Pennsylvania, 1999.

22. S.V. Patankar, *Numerical Heat Transfer and Fluid Flow*, McGraw Hill, New York, 1980.

23. E. Polak, *Computational Methods in Optimization*, Academic Press, New York, 1971.

24. A.N. Tikhonov and V.Y. Arsenin, *Solution of Ill-posed Problems*, Winston and Sons, Washington D.C., 1977.

25. H. Zheng and D.A. Murio, A stable algorithm for 3D-IHCP. *Comput. Math. Appl.* (1995) **29**(5), 97-110.

26. H. Zheng and D.A. Murio, 3D-IHCP on a finite cube. *Comput. Math. Appl.* (1996) **31**(1), 1-14.